Geosci. Model Dev. Discuss., 7, 5295–5340, 2014
www.geosci-model-dev-discuss.net/7/5295/2014/
doi:10.5194/gmdd-7-5295-2014

Geoscientific
Model Development
Discussions
Open Access

Predicting the response of the Amazon rainforest to persistent drought conditions under current and future climates: a major challenge for global land surface models

E. Joetzjer[1], C. Delire[1], H. Douville[1], P. Ciais[2], B. Decharme[1], R. Fisher[3], B. Christoffersen[4], J. C. Calvet[1], A. C. L. da Costa[5], L. V. Ferreira[6], and P. Meir[7]

[1]CNRM-GAME UMR3589, Groupe d'étude de l'atmosphère météorologique, Toulouse, France
[2]LSCE UMR 8212, Laboratoire des Sciences du Climat et de l'Environnement, Gif-sur-Yvette, France
[3]NCAR National Center for Atmospheric Research, Boulder, Colorado, USA
[4]School of GeoSciences, University of Edinburgh, Edinburgh, UK
[5]Universidade Federal de Para, Belem, Para, Brasil
[6]Museu Paraense Emilio Goeldi, Belem, Para, Brasil
[7]Australian National University, Canberra, Australia

Received: 3 July 2014 – Accepted: 18 July 2014 – Published: 8 August 2014

Correspondence to: E. Joetzjer (emilie.joetzjer@meteo.fr)

Published by Copernicus Publications on behalf of the European Geosciences Union.

Abstract

While a majority of Global Climate Models project dryer and longer dry seasons over the Amazon under higher CO_2 levels, large uncertainties surround the response of vegetation to persistent droughts in both present-day and future climates.

We propose a detailed evaluation of the ability of the $ISBA_{CC}$ Land Surface Model to capture drought effects on both water and carbon budgets, comparing fluxes and stocks at two recent ThroughFall Exclusion (TFE) experiments performed in the Amazon. We also explore the model sensitivity to different Water Stress Function (WSF) and to an idealized increase in CO_2 concentration and/or temperature.

In spite of a reasonable soil moisture simulation, $ISBA_{CC}$ struggles to correctly simulate the vegetation response to TFE whose amplitude and timing is highly sensitive to the WSF. Under higher CO_2 concentration, the increased Water Use Efficiency (WUE) mitigates the $ISBA_{CC}$'s sensitivity to drought.

While one of the proposed WSF formulation improves the response of most $ISBA_{CC}$ fluxes, except respiration, a parameterization of drought-induced tree mortality is missing for an accurate estimate of the vegetation response. Also, a better mechanistic understanding of the forest responses to drought under a warmer climate and higher CO_2 concentration is clearly needed.

1 Introduction

The Amazon rainforest biome plays a crucial role in the global climate system regulating the regional energy, water and carbon cycles, and thereby modulating the tropical atmospheric circulation. The forest recycles about 25 to 35 % of the Amazonian precipitation through evapotranspiration (Eltahir and Bras, 1994) and stores about 10 to 15 % of the global above ground biomass (e.g. Potter, 1999; Mahli et al., 2006; Beer et al., 2010; Pan et al., 2011).

The vulnerability of the Amazon forest to climate change is of great concern, especially as climate projections based on the fifth phase of the Coupled Model Intercomparison Project (CMIP5) show a between-model consensus towards dryer and longer dry seasons in this region (Fu et al., 2013; Joetzjer et al., 2013). Beyond this model consensus, however, substantial uncertainties in the current assessments given uncertainty in climate feedbacks and climate sensitivity to anthropogenic forcing remain. They arise from many sources including the limited ability of coupled ocean–atmosphere general circulation models (OAGCMs) to capture the present-climate global patterns of temperature and precipitation as well as local vegetation-climate feedbacks (Jupp et al., 2010; Shiogama et al., 2011).

Land surface feedbacks also represent a significant source of uncertainties for climate projections over the Amazon basin (Meir et al., 2006; Friedlingstein et al., 2006; Poulter et al., 2009; Rammig et al., 2010; Galbraith et al., 2010; Booth et al., 2012). This was highlighted by the large spread in the future Amazonian evapotranspiration response to climate change among CMIP5 models (Joetzjer et al., 2013) and the growing evidence that global evapotranspiration has already been perturbed by human activities (Douville et al., 2013), a process which could contribute to increase drought hazards in many areas during the 21st century. About half of the CMIP5 models are Earth System Models (ESMs) that simulate the global carbon cycle and account for direct CO_2 effects on plants such as an increased water use efficiency (WUE) due to both photosynthesis (i.e. fertilization effect) and stomatal closure responses to increasing atmospheric CO_2 concentrations. Given their diversity and their limited ability to capture biophysical mechanisms (e.g. Keenan et al., 2013), a process-oriented evaluation of the current-generation land surface models (LSM) is needed.

In this paper, the emphasis is on the Amazon forest response to persistent soil moisture deficit in both observed present-day and idealized future climates. Such a focus is justified not only by the enhanced dry seasons found in most CMIP5 climate scenarios, but also by the possible though uncertain “dieback” of the Amazon rainforest in some projections (Cox et al., 2000, 2004; Galbraith et al., 2010; Good et al., 2013;

Huntingford et al., 2013). Drought is likely to perturb biogeochemical cycles and to stress vegetation and to disturb CO_2 fluxes as well as to cause carbon stock reductions due for instance to increased plant mortality (van der Molen et al., 2011; Reichstein et al., 2013). As observed during the 2010 Amazonian drought, the net CO_2 net uptake by a large area of the Amazon forest was reduced (Gatti et al., 2014). Severe droughts can also lead to tree damage, causing mortality and increased fire hazards (Nepstad et al., 2004; Phillips et al., 2009; Anderson et al., 2010), therefore reducing the carbon sink capacity of the Amazonian biome (Fisher et al., 2007; Mahli et al., 2008; Phillips et al., 2009; Lewis et al., 2011). Before the end of the 21st century, the Amazon forest should experience not only a drier climate with longer dry seasons, but also higher atmospheric temperatures and elevated global CO_2 concentration, with potential non-linear effects on the water and carbon exchanges within the soil-plant-atmosphere continuum (Berry et al., 2010).

Besides interannual climate variability, field experiments impacting precipitation can be used to study the vegetation response and evaluate LSMs sensitivity to persistent drought conditions at the plot scale. This was one aim of the two throughfall exclusion (TFE) experiments carried out in the eastern Amazon (at the National forest reserves of Tapajós and Caxiuanã, in eastern Amazonia) during the Large-Scale Biosphere–Atmosphere Experiment in Amazonia (LBA) (Nepstad et al., 2002; Meir et al., 2009; da Costa et al., 2010). Such field experiments are extremely useful to assess and improve the parameterization of hydrological, carbon and other ecosystem processes in LSMs (Galbraith, 2010; Sakaguchi et al., 2011; Powell et al., 2013). In particular, the simultaneous availability of soil moisture, sap flow and photosynthesis measurements provides a unique opportunity to evaluate the Water Stress Function (WSF) used in such models to represent the soil moisture effect on plants' stomatal conductance (Powell et al., 2013).

In this study, we first briefly describe the $\mathrm{ISBA_{CC}}$ LSM developed at CNRM (Centre National de Recherches Météorologiques, Toulouse, France) and the in situ observations that have been collected at the two TFE experimental sites (Sect. 2). We then conduct a detailed evaluation of the ability of the ISBA_{CC} LSM to capture drought effects on both water and carbon budgets, comparing fluxes and stocks at the TFE vs. control sites (Sect. 3). We explore the model sensitivity to the WSF parameterization and to an idealized increase in CO_2 concentration and/or temperature in the prescribed atmospheric forcings. Finally, we discuss the implications of our results for modeling the Amazon rainforest sensitivity to climate change in Sect. 4 and draw the main conclusions of the study in Sect. 5.

2 Model, observations and methods

2.1 ISBA_{CC}

2.1.1 Model description

The ISBA (Interaction Soil Biosphere Atmosphere, Noilhan and Planton, 1989; Noilhan and Mahfouf, 1996) Land Surface Model computes the exchanges of water and energy between the land surface and the atmosphere. In order to account for the interactions between climate and vegetation, Calvet et al. (1998) implemented a carbon assimilation scheme (A-gs). ISBA-A-gs does not explicitly account for enzyme kinetics but instead employs a semi-empirical response function which distinguishes between CO_2 and light-limited regimes, following the approach of Jacobs (1995). The effects of temperature on photosynthesis arise from the temperature dependencies of the CO_2 compensation point (Γ), mesophyll conductance (g_{m}), and the maximum photosynthetic rate ($A_{\text{m, max}}$) via standard Q_{10} response functions. The standard ISBA-A-gs equations describing these dependencies are given in Calvet et al. (1998) and Gibelin et al. (2006), and those relevant to the drought response are given in Table 1 and described below. The A-gs scheme only accounts for the evolution of leaf assimilation and biomass. Gibelin et al. (2008) introduced a C-allocation scheme and a soil carbon module to represent the other pools and fluxes of carbon in the plant and in the soils.

This latest version, called ISBA$_{CC}$ (ISBA Carbon Cycle) is used in this study. To better simulate soil moisture content in the deep Amazonian soils we use the multilayer soil diffusion scheme implemented in ISBA and described by Decharme et al. (2011) and Decharme et al. (2013). In addition, the canopy radiative transfer scheme developed by Carrer et al. (2013) is used.

The ISBA$_{CC}$ photosynthesis model relies on the concept of mesophyll conductance (g_m). As defined by Jacobs (1995), g_m quantifies the slope of the CO$_2$ response curve at high light intensity and low internal CO$_2$ concentration (C_i) and can be interpreted as a parameter to model the activity of the Rubisco under these conditions (Table 1 Eq. 1). ISBA$_{CC}$ uses a constant unstressed value of g_m (g_m^*) per vegetation functional type (PFT). ISBA$_{CC}$ also defines a ratio f which relates C_i to ambient CO$_2$ (C_a) (Table 1 Eq. 2), and (Table 1 Eq. 3) posits a linear decrease in the coupling factor f (and hence, C_i) with increasing atmospheric humidity deficit (Table 1 Eq. 3). Assimilation is calculated from light, air humidity, C_a, the ratio of C_i/C_a and finally, g_s is deduced from the assimilation rate. The sensitivity of g_m to the soil water availability is quantified by a water stress function (WSF), as explained below.

2.1.2 Water stress functions

The water stress function (WSF) is an empirical formulation of the effect of soil moisture stress on transpiration and photosynthesis. In the case of ISBA$_{CC}$, soil water content (SWC) affects transpiration and photosynthesis through changes in g_m and/or f_0, depending on the PFT and its drought strategy (Table 2). We test two plant strategies which were proposed by Calvet et al. (2004) for responding to soil moisture stress, as represented in Fig. 1. The *drought-avoiding* strategy, corresponding to the curve in blue, attempts to represent *isohydric* plants. The *drought-tolerant* response of *anisohydric* plants is represented in purple in Fig. 1. However, these parameterizations were derived from measurements made on saplings of *Pinus pinaster* and *Quercus petraea* (Picon et al., 1996), and have not been calibrated for matures trees nor for tropical species. Also, for tropical rainforests, photosynthesis and transpiration simulated in

ISBA$_{\mathrm{CC}}$ are highly sensitive to the value of f_0 because the air is often close to saturation. Therefore, and in addition to the physiologically-based drought-avoiding and drought-tolerant WSF parameterizations existing in ISBA, we also tested two simpler WSFs: a linear and the SiB3 formulation documented in (Baker et al., 2008). We applied both of these WSFs to g_{m}. These functions assume a constant f_0 derived from in situ observations (Table 2, Domingues et al., 2007)

The Soil Wetness Index (SWI) quantifies the soil moisture condition. It is defined as:

SWI = $(\theta - \theta_{\mathrm{wilt}})/(\theta_{\mathrm{fc}} - \theta_{\mathrm{wilt}})$; so at field capacity ($\theta = \theta_{\mathrm{fc}}$;), SWI = 1 and at wilting point ($\theta = \theta_{\mathrm{wilt}}$), SWI = 0.

At field capacity, due to a higher f_0, the linear and SiB3 WSF are alternative parameterizations that allow a larger stomatal conductance in line with a higher GPP and a higher evapotranspiration than both drought-tolerant and avoiding WSF shown in Fig. 1. In spite of a quite similar response between the linear and the drought tolerant WSF on the one hand, and between the SiB3 and drought avoiding WSF on the other, when looking at the response of g_{m} to soil moisture deficit (Fig. 1), the linear and SiB3 WSFs induce a stronger response to drought (Fig. 1) because they do not influence f_0^*.

2.2 Site description and observations

Two rainfall exclusion experiments were initiated at national forests of Tapajós (2.90° S, 54.96° W) and Caxiuanã (1.72° S, 51.46° W) in 1999 and 2001 respectively. At each site, the experimental design consists of a 1-hectare forest undisturbed control plot (CTL) and in a nearby floristically and structurally similar 1 ha forest plot from which a portion of throughfall was excluded (TFE) using large plastic panels below the canopy, approximately 1–2 m above the ground. A 1 m deep trench was dug around each plot to minimize lateral movement of water and roots. Panels were applied 1 yr after the beginning of the experiments to assess pre-treatment plot differences. At Tapajós (Caxiuanã), 1999 (2001) was the baseline year, and the TFE experiment lasted from 2000 until 2004 (2002 and remains ongoing). At Tapajós, panels were removed during the dry season (Fig. 1) to reduce their influence on the forest floor through shading and heating. It was estimated that panels increased forest floor temperature by no more than 0.3 °C (Nepstad et al., 2002). At Caxiuanã panels were not removed because the risk of dry season storms is relatively high at that site; the air temperature below the TFE panels was no different from ambient during the wet season, and varied up to 2 °C warmer during the dry season; soil temperature differences in TFE remained similar to ambient throughout (Metcalfe et al., 2010).

While soils at both sites are highly weathered oxisols, they differ greatly in texture. Caxiuanã is a sandy soil and presents a stony laterite layer at 3–4 m deep which could hamper deep roots development and soil water movement (Fisher et al., 2007), contrasting with the clay rich soil at Tapajós. Besides, the water table depth is > 80 m (Nepstad et al., 2002) at Tapajós while it reaches 10 m at Caxiuanã during the wet season (Fisher et al., 2007). Caxiuanã shows also a wetter climate (more precipitation and longer wet season) than Tapajós (Fig. 2).

A large suite of observations was provided to understand the response of the Amazon forest to these two rainfall experiments (Meir et al., 2009). Observations used in this study to evaluate ISBA$_{\text{CC}}$ are summarized in Table 3 with the associated references. There is no direct measurement of LE as fluxtowers have a spatial footprint of about 1 to 10 km^2, much larger than the size of the experiments (Cheng et al., 2008), and GPP can only be inferred from adding up respiration and NPP (Net Primary Productivity) terms, or modelled. We use as a reference, evapotranspiration outputs from a 1-D model calibrated and validated at Tapajós from Markewitz et al. (2010, Table 5) and the GPP estimated at Caxiuanã by Fisher et al. (2007); both fine-scale model outputs were carefully and successfully validated using datasets independent from those used to specify the model structure.

2.3 Simulations

At both sites, ISBA$_{\text{CC}}$ was run off-line using in situ hourly meteorological measurements made above the forest canopy at nearby weather stations (also available at http://beija-flor.onrl.gov/lba). At Caxiuanã meteorological measurements were available for the entire experimental period (2001–2008), at Tapajós they covered only the years 2002 to 2004. To cover the entire period of experimentation, we cycled sequentially the available years. ISBA$_{\mathrm{CC}}$ was run until the slowest soil storage pools of water and carbon had reached equilibrium.

ISBA explicitly simulates interception of precipitation by the canopy and throughfall as runoff from the leaves. To simulate the experimental treatments at each experiment we removed 60 % of the throughfall in our model runs. This is consistent with Markewitz et al. (2010) and Sakaguchi et al. (2011) for Tapajos, and similar to the 50 % exclusion of incident (above-canopy) rainfall implemented at Caxiuanã (Fisher et al., 2007; Galbraith et al., 2010; Powell et al., 2013). The 60 % reduction of throughfall was applied to the entire period at Caxiuanã (2001–2008) and only during the rainy seasons (January to June) from 2000 to 2004 at Tapajós, to mimic the experimental conditions.

At both sites, we imposed the "evergreen tropical tree" plant functional type. To better represent the soil moisture and focus on vegetation response, we constrained ISBA$_{\mathrm{CC}}$ using the observed texture at each site. The soil texture values used for the simulations are, at Caxiuanã 75 % sand and 15 % clay (Ruivo and Cunha, 2003) and 52 % sand and 42 % clay at Tapajós following the LBA-Data Model Intercomparison Project (www.climatemodeling.org/lba-mip). To mimic deep amazonian soils, soil and root depth were fixed at 8 m at both sites, even at Caxiuanã, because roots were found below the laterite layer located at 3–4 m deep (Fisher et al., 2007). Considering deep soil and roots may avoid the simulation of unrealistic responses to drought due to a drying of the upper layers (Baker, 2008) although Guimberteau et al. (2014) found that in a soil diffusion model, the sensitivity of soil moisture to soil depth was smaller than in a bucket model (Verbeeck et al., 2011) because a multilayer scheme tends to retain more water in the soil during the dry seasons. Note that the same soil texture is used in all the model soil layers, which has little impact when simulating 1 m soil depth (Sakaguchi et al., 2011). However when considering deeper soils, it would be better to set soil texture per layer, which, according to our knowledge, could not be done due to a lack of published observations. For instance we could not represent the laterite layer at Caxiuanã. To overcome this issue, a exponential vertical profile decreasing with depth was applied to the hydraulic conductivity to represent the increasing bulk density (Decharme et al., 2006).

Throughfall exclusion experiments are not fully representative of future climate conditions. Besides more severe and persistent dry seasons, atmospheric CO_2 concentrations will increase as well as near-surface air temperature and VPD. Therefore we chose to analyze how the model sensitivity to drought can be affected by increased CO_2 concentration and increased temperature. In line with the idealized CMIP5 climate change experiments, we tested arbitrary high values of CO_2 and temperature in the model with the same TFE as observed: 4 times the preindustrial CO_2 concentration (1080 ppmv), +4 °C greater (higher) temperature, and a combination of both. The CO_2 concentration and the increase in temperature are constant year round. We did not modify the specific humidity, but a 4 °C arbitrary warming lowers the relative humidity and increases the evaporative demand of the atmosphere. The simulations are summarized in Table 3.

3 Results

3.1 Hydrological response

$ISBA_{CC}$ simulates the SWC and its seasonality fairly well between 0–3 m (Fig. 3) at both sites for the CTL plots, but the model tends to be too wet during the dry season. The low correlations (around 0.65) between observations and simulations at Tapajós are potentially due to the use of reconstructed forcing data, that was necessary to cover the entire experimental period. Despite a wetter climate (Fig. 2), the simulation at Caxiuanã produces a drier soil, in line with a sandier texture. Due to higher evapotranspiration, the SiB3 and linear WSF slightly improve the simulations of SWC, including the seasonality, reducing the wet bias and improving the correlations at both sites compared to the original functions. When throughfall exclusion is applied to the model, the observed reduction in SWC is also better captured by the Linear and the SiB3 WSF than by the avoiding and tolerant WSF functions, since they result in a stronger negative response to drought (Fig. 3, lower panels). There is little difference of SWC between the linear and SiB3 WSF.

The full daily times series of the simulated SWI for both CTL and TFE plots are plotted in Fig. 4 to better compare the hydrology at the two sites and to illustrate how variations in soil moisture translate into water stress in the model. With 60 % of the throughfall removed to mimic the TFE (not during the dry season at Tapajos), the SWI remains close to one (field capacity) with the drought-avoiding and tolerant WSFs while it drops below 0.5 with the linear and Sib3 WSFs. The unstressed transpiration fluxes (at $\text{SWI} > 1$) are lower with the drought-avoiding and tolerant WSFs and the soil moisture is not depleted quickly enough. Therefore the edaphic water stress isn't captured and we expect little impact on the vegetation fluxes. With the linear and SiB3 WSF, the SWI clearly decreases, imposing a strong hydrological stress, mainly with SiB3, as the SWI is getting close to zero (wilting point).

3.2 Vegetation response

3.2.1 Water and carbon budget

To understand the response of ISBA_{CC} to drought, we compare the density functions (Fig. 5) of daily SWI, g_s, GPP and LE for the dry (August to October) and the wet seasons (February to April) over 2000–2005 at Tapajós and 2001–2009 at Caxiuanã, for the CTL and TFE plots. Note that as the drough-avoiding and tolerant WSFs showed a very similar behavior, only the Avoiding WSF was plotted.

In the CTL plot (solid lines), at both sites and for all WSF, the modeled values of g_s, LE and GPP are higher during the dry season than during the wet season following the higher available energy, in line with less clouds, more solar radiation, less precipitation and an enhanced evaporative demand. Now, looking at the different WSF, in both seasons, the stomatal conductance is higher with the linear and SiB3 WSF (Fig. 1) which enhances LE and GPP. Using linear and SiB3 WSF also results in a stronger response to drought than using the drough-avoiding and tolerant WSFs. Therefore, during a drought (dashed lines and shaded areas), the distribution of SWI is shifted towards lower values with SiB3 and linear WSFs compared to the original WSF. Indeed, with the tolerant (and avoiding) WSF, the SWI remains above 0.5, even during TFE, whichever season is considered. Therefore the simulated vegetation response to TFE for these WSF is rather weak.

At Caxiuanã, the reduction of SWI during TFE is more pronounced than at Tapajós, consistent with the sandier soil and the longer experiment. The strongest responses of the carbon and water happen during the dry season, when the soil moisture content drops close to wilting point revealing the high sensitivity to soil moisture content, and therefore to the seasonality in ISBA_{CC}. Also, the response is more pronounced with the Linear and the SiB3 WSF than with the original functions, and, at Caxiuanã than at Tapajós.

As the modelled carbon and water response to drought are mainly driven by the stomatal response to drought, Fig. 6 shows the seasonality of the simulated and observed hourly stomatal conductance at Caxiuanã for a few days for the control and the TFE. All models underestimate wet season g_s in both plots, particularly with the tolerant and avoiding WSF. The dry season observations are better captured, and at both sites, all models appear to be within the range of the observations which themselves span across a range of species, and thus show significant spread. However, and despite the high spread between observed g_s values, the response to drought seems to be underestimated by all WSF except when soil moisture becomes extremely limited (TFE and dry season). Note that the g_s simulated whith the linear WSF is the most reactive to drought.

Moving to annual fluxes (Fig. 7), for all water stress functions, ISBA_{CC} simulates some decrease in LE and GPP between the CTL and TFE plots. The Linear WSF predicts a larger decline in LE and GPP, which is closer to observation-constrained estimates at both sites (Fisher et al., 2006, 2007; Markewitz et al., 2010). The SiB3

WSF allows a higher transpiration rate than the Linear function for the same intermediate SWC (Fig. 1), depleting the soil water faster, and giving a later but much stronger response to drought at Caxiuanã.

Figure 8 shows the difference between TFE and CTL of the measured daily sap flow and the simulated daily transpiration using the linear WSF. While they can not be quantitatively compared, the sap flow measurements are a good proxy to evaluate the seasonality of the transpiration. The model simulates reasonably well the seasonality of the reduction in transpiration induced by TFE. Note that only the simulation using the linear WSF is plotted in Fig. 8, as transpiration simulated with other WSFs greatly differ in amplitude but not in seasonality.

3.2.2 Autotrophic and heterotrophic respiration

We compared the model output to estimates of ecosystem carbon fluxes derived by Metcalfe et al. (2010) at Caxiuanã. The model overestimates woody tissue respiration and underestimates respiration of leaves and roots. These errors compensate each other and overall the ISBA$_{CC}$ reasonably matches the yearly heterotrophic and autotrophic respiration fluxes at Caxiuanã (Fig. 9, CTL). This result remains valid over several sites across the Amazon watershed when comparing ISBA$_{CC}$ to the dataset compiled by Malhi et al. (2009) (not shown).

At Caxiuanã, whole ecosystem respiration was observed to increase during the TFE experiments mainly attributable to a temperature corrected enhanced leaf respiration rate per unit LAI (Metcalfe et al., 2010), as also observed during seasonal drought elsewhere in the Amazon (Miranda et al., 2005). One hypothesis to explain this observation is that the enhanced respiration may supply the supplementary energy demand induced by drought to actively maintain the gradients of the vacuolar solute to keep a minimum turgor (osmotic adjustment) and/or to repair water stress induced cell damage (Metcalfe et al., 2010; Atkin and Macherel, 2009 and references within).

In contrast to the observations, ISBA$_{CC}$ predicts a decrease of the autotrophic respiration with drought that is not balanced by the increase in vegetation temperature due to the decrease in latent heat production (which reaches a maximum of 2 K during the driest dry season). The ISBA_{CC} model, in common with the majority of ecosystem models, couples autotrophic respiration to assimilation, and implicitly to the LAI, and therefore declines during drought. As the heterotrophic respiration is a function of the soil water content, the reduction of Rs induced by drought is underestimated at Caxiuanã (Sotta et al., 2007), but at least, the sign is in agreement with observations.

3.2.3 Biomass carbon stocks

The simulated daily LAI compares reasonably well with the in situ observation at both control sites (Fig. 10). The SIB3 and linear WSFs result in LAIs a little higher than the tolerant and avoiding WSFs (in line with a higher gs and GPP, seen in Fig. 1). At Tapajós, ISBA_{CC} underestimates LAI in 2000 and 2001, which might be explained by the reconstructed forcing for these years missing variation in the meteorological conditions that might have promoted higher LAI. At Caxiuanã the anomalously low LAI value (4 $\text{m}^2.\text{m}^{-2}$) measured in November 2002 is not captured by the model.

ISBA_{CC} fails to simulate the observed substantial loss of LAI (from 1 to 2 points, about 20 % of leaf area, Meir et al., 2009) during TFE at both sites. With the tolerant and avoiding WSFs, the soil water content remains above field capacity (SWI > 1, Fig. 4) at both sites, there is almost no hydrological stress, and the simulated LAI shows no response to drought. When using the linear or SiB3 WSF, the loss of LAI remains underestimated at Tapajós, where the SWI remains relatively high compared to Caxiuanã (Fig. 4). At Caxiuanã, the observed LAI in the TFE experiment diverged from the control within 2 years by more than one LAI unit. There are no LAI measurements between 2004 and 2007. The model underestimates the early LAI decrease consecutive to TFE in 2003 with all the WSFs. From the end of 2005 through 2007, the SiB3 WSF results in strong and rapid decreases of LAI during the dry seasons followed by rapid recovery during the wet seasons, partly driven by the the strong seasonality of the soil moisture which almost reaches the wilting point during each dry season after 2005 (Fig. 4).

Although there were no LAI observations in 2005 and 2006, it is likely that this 4 point decrease of simulated LAI is too strong, and the speed of the recovery is not realistic. The fast changes in modelled LAI (Fig. 10) showing little memory of previous droughts are coherent with the model's hypothesis that the LAI is driven by current assimilation. With the linear WSF, the model's behavior is closer to the reality because the SWC remains higher and the vegetation shows a smoother response to drought.

Above-ground biomass observations at Caxiuanã show a reduction of stand-level biomass by 20 % after 7 years of TFE, mainly due to enhanced tree mortality. The model predicts AGB in the CTL plot with some skill, but the loss of AGB in the TFE is strongly underestimated with the Linear and SiB3 WSF, and not captured at all with the original WSF (Fig. 11). This result is not surprising since ISBA$_{CC}$ only represents background turnover rates depending on biomass stocks and fixed turnover times. There is no representation of mortality processes driven by plant physiology or strong climate anomalies.

3.3 Drought response sensitivity to background temperature and CO$_2$

Figure 12 shows simulated monthly LE and GPP against monthly SWI computed at Caxiuanã over the whole 2001–2008 period, with the linear WSF forced by the original forcing and by three modified meteorological forcings (Table 3). Under a warmer climate (+4 K), the higher evaporative demand increases LE, and the model becomes more sensitive to drought. Conversely, ET is strongly reduced when imposing a high CO$_2$ concentration due to increased water use efficiency (WUE) because stomata need to be less open, therefore reducing transpiration for the same CO$_2$ uptake (Woodward, 1987; Lloyd and Farquhar, 2008). Consequently ISBA$_{CC}$'s sensitivity to the experimental drought is completely dampened. The SWI remains close to or above 1 even when removing 60 % of the incoming throughfall (red dots).

The GPP is barely impacted by the +4 K in the CTL plot as the temperature is already close to the assimilation optimum temperature, but is limited in the exclusion plot due to the stronger water stress linked with temperature-induced higher evaporation rates.

Maximum GPP increases by about 50 % under 4 × CO_2 because of the fertilization effect. Indeed under higher CO_2 concentration, the CO_2 diffusion into the mesophyll is easier, therefore enhancing the carboxylation rate (Lloyd and Farquhar, 2008 and references within). Merging the two treatments (+4 K and 4 × CO_2), the higher evaporative demand balances the increased WUE and leads the model to simulate a soil moisture deficit. Note that using the SiB3 SWF leads to similar patterns (not shown) indicating that the strong environmental changes imposed here dominate the model's sensitivity to drought.

4 Discussion

4.1 Water stress functions

The drought-avoiding and tolerant strategies originally implemented in ISBA_{CC} are not effective at simulating gas exchange fluxes when running the model over the Amazon forest, even when the soil moisture is not limiting. This conclusion is very likely to remain valid for other tropical forests and further studies need to assess their validity at global scale. Also, even if the original WSF meant to represent isohydric and anysohydric drought responses, their results are not consistent with physiological observations since there is little difference in transpiration between both strategies due to a fo compensation effect. The linear WSF is more suitable for ISBA_{CC} but, as the WSF is applied to g_m and not to g_s, the response to drought of g_s is not linear (Fig. 1). The SiB3 WSF responds too strongly to drought as it is applied to g_m in ISBA_{CC} (and not to g_s as in SiB3).

The difference in timing and amplitude of the vegetation response to drought when using the linear and SiB3 WSFs illustrate the model sensitivity to the chosen WSF. The WSF parameterization is also likely to be site dependent making the WSF modeling more challenging. However, the formulation of the WSF greatly differs from one land surface model to another (Egea et al., 2011; Zhou et al., 2013) reflecting our inability to define the general behavior(s) of a multi-specific biome while the physiological processes are not yet fully understood. The use of "hydrodynamic" models, that do not include empirical soil moisture response functions, but instead predict drought-induced stomatal closure from the simulation of hydraulic potential in the continuum soil-plant-atmosphere, has demonstrated some promising results (Williams et al., 2001; Fisher et al., 2006, 2007; Zeppel et al., 2008; McDowell et al., 2013).

4.2 Respiration

Despite measurement uncertainties, leaf respiration at Caxiuanã increases significantly with drought (Metcalfe et al., 2010), a process which is not captured by ISBA$_{\text{CC}}$. Other LSMs exhibit the same behavior as shown by the multi-model comparison against the TFE data (Powell et al., 2013). Although a decrease in leaf dark respiration is usually observed when photosynthetic capacity declines under drought, increases in leaf dark respiration have been observed elsewhere (Metcalfe et al., 2010; Atkin and Macherel, 2009), including elsewhere in Amazonia during seasonal drought (Miranda et al., 2005). As asked by Powell et al. (2013), are we missing a critical physiological process to accurately compute the plant carbon balance during drought? Perhaps, but whatever the sign of the response, the changes in respiration tend to be smaller than the decrease in carbon assimilation when in drought (Atkin and Macherel, 2009).

4.3 Mortality

The inability to simulate drought-induced tree mortality highlighted by the TFE is expected from a compartment carbon model such as ISBA$_{\text{CC}}$ that has no deterministic climate–mortality relationship. It also concerns LSMs linking mortality to negative carbon balance through the carbon starvation hypothesis (da Costa et al., 2010; Powell et al., 2013; McDowell et al., 2013). Mortality driven by climate and especially drought since it is a significant driver of mortality (da Costa et al., 2010; Allen et al., 2010), is a required process to implement in LSMs to assess the resilience of the Amazon forest under climate change and to reasonably estimate vegetation feedbacks when running LSMs coupled with global climate models.

Mortality is a complex process, highly non linear in both time and space (Allen et al., 2010; Fisher et al., 2010; McDowell, 2011). Unfortunately as ISBA$_{CC}$, like most LSMs, does not account for the water column pressure within the xylem, the drought induced cavitation process cannot be represented. Besides, increased mortality risk during drought is associated with other processes like fire or insect outbreaks. Therefore mortality is not yet fully understood, and commonly used LSMs use a wide array of algorithms to represent plant mortality (McDowell et al., 2013). Throughfall exclusion experiments should therefore be used in combination with other datasets, rather than used alone to imporove the mortality response to drought in LSMs. The results from the experiments contain uncertainty in the impact on biomass over 1 ha, particularly as it is the bigger trees that tend to die first (in both the experiments and in natural droughts; Nepstad et al., 2007; Meir et al., 2009; Phillips et al., 2010), although at Caxiuanã baseline mortality rates in the experiment were strongly consistent with data from multiple nearby monitoring plot, adding confidence to the observed mortality impacts. However, the detailed longitudinal datasets and the control over soil moisture that these experiments offer yield insights into ecological processes and dynamics that are not available from forest inventory datasets, and yet are crucial for validating the processes represented by DGVMs. Therefore, a combination of data sources seems the most effective way forward to constrain and evaluate forest demography and ultimately biomass within LSMs, and its sensitivity to climate, for example through using data from long term inventory plots such as those from (French Guyana) since 1991, the RAINFOR datasets in Amazonia (Phillips et al., 2009) or trait-based mortality model outputs (e.g. Aubry-Kientz et al., 2013), as well as the detailed results from the throughfall exlusion experiments.

4.4 Drought responses changes under different background conditions

Increases in CO_2 and temperature are modeled to have antagonistic effects on soil moisture through evapotranspiration because the WUE increases under higher CO_2 concentration (reducing transpiration) while higher temperature will enhance transpiration though a higher vapor pressure deficit. The simulated ET is highly reduced when imposing a high CO_2 concentration and $ISBA_{CC}$'s sensitivity to TFE is completely dampened. Unfortunately, there are no direct observations of the response to elevated CO_2 in tropical forests with which to constrain the reduced transpiration effect implemented in $ISBA_{CC}$ (and in other LSMs). The disputed increasing global runoff over the past 50 years, attributable to CO_2 induced stomatal closure (Gedney et al., 2006; Betts et al., 2007), or more recently, the strong positive trend of WUE deduced from 21 fluxtowers (Keenan et al., 2013) over the past two decades, can not really be used as proxies. Nevertheless, projections are highly sensitive to the response of the stomatal closure to a CO_2 enrichment (Cowling et al., 2008; Good et al., 2013; de Kauwe et al., 2013). If, as recently suggested in Keenan et al. (2013), LSMs tend to underestimate CO_2 induced stomatal closure, it is likely that increasing WUE will partly offset future droughts, and mitigate the dryer and longer expected dry season (Fu et al., 2013). Therefore, the stomatal response, which regulates the water exchange within the soil-plant-atmosphere continuum, is fundamental to modelling the vegetation response to climate change (Berry et al., 2010). On the other hand, less ET reduces the water flux towards the atmosphere, the local evaporative cooling, and might reduce precipitation through vegetation-atmosphere feedbacks. Numerous global climate model simulations of deforestation in the Amazon showed that regional precipitation is expected to decrease because of the combined influences of increased albedo, decreased surface roughness and decreased water recycling that accompany deforestation (Dickinson and Henderson-Sellers, 1988; Malhi et al., 2008; Coe et al., 2009). Increased WUE is obviously not equivalent to deforestation since it does not affect albedo or surface roughness but will affect the whole basin while deforestation won't.

5 Conclusions

Accurate representation of soil moisture and its seasonal dynamics is a prerequisite to simulate drought impacts on vegetation. However, in spite of a reasonable hydrology, ISBA$_{CC}$ fails to correctly simulate the vegetation response to the two Amazon rainfall exclusion experiments. First, a sensitivity analysis based on four WSFs showed that the amplitude and timing of ISBA$_{CC}$'s vegetation response to drought is quite sensitive to the WSF chosen. The drought-avoiding and tolerant strategies originally implemented in ISBA$_{CC}$ are not suitable for the Amazon forest on account of a g_s significantly lower than that observed. Of the functions we tested, the simplest linear function performs best.

While at Caxiuanã, the measured autotrophic respiration tends to be higher in the TFE than in the CTL plot, ISBA$_{CC}$ simulates an opposite trend. The observed loss of AGB, hiding the drought enhanced tree mortality, was greatly underestimated or even not captured by the model, as it does not represent mortality driven by strong climate anomalies.

If there is no edaphic stress, the representation of the vegetation (in terms of fluxes and stocks) is quite well simulated by ISBA$_{CC}$ but, physiological processes are missing to correctly estimate the vegetation response in case of drought. We also showed that the vegetation response to higher CO$_2$ and warmer temperature greatly affects its response to drought. As discussed, this can have great impacts to estimate the Amazon response to climate change and the vegetation feedbacks in climate projections.

Land surface models are designed to conduct investigations of processes with large spatial and temporal scales, and therefore, the vegetation representation necessarily includes many empirical approximations and coarse abstractions of reality. The definition of a generic drought response for Amazonian forests in evidently a difficult undertaking, particularly given evidence of the functional diversity of these forests in hydraulic functioning alone (Fisher et al., 2006; Baraloto et al., 2009). The introduction of more complex mechanistic models of drought stress removes the requirement to generate these empirical functions, but implies significantly higher model complexity and requirements for model specification using data that are difficult to acquire (root density, soil hydraulic conductivity, xylem conductance, etc.). The optimal strategy for drought simulation in land surface models remains unclear at this time. Further to this, better mechanistic understanding of the forest responses to drought under a warmer climate and higher CO_2 concentration is clearly needed, as some physiological processes are not yet fully understood and/or little observations are available, to improve LSMs.

Acknowledgements. The authors are grateful to Colin Prentice, Jerôme Chave, Lawren Sack, Bruno Hérault, David Galbraith, Paulo Brando and Daniel Markewitz for helpful discussions and/or for providing datasets. P. Meir acknowledges support from ARC FT FT110100457 and NERC NE/J011002/1. Thanks are also due to the AMAZALERT FP7 project for supporting this study.

References

Allen, C. D., Macalady, A., Chenchouni, H., Bachelet, D., McDowell, N., Vennetier, M., Gonzales, P., Hogg, T., Rigling, A., Breshears, D., Hogg, E. H. (Ted), Gonzalez, P., Fenshaml, R., Zhangm, Z., Castro, J., Demidovao, N., Limp, J. H., Allard, G., Runningr, S. W., Semerci, A., Cobbt, N.: Climate-induced forest mortality: a global overview of emerging risks, Forest Ecol. Manag., 259, 660–684, doi:10.1016/j.foreco.2009.09.001, 2010.

Anderson, L. O., Malhi, Y., Aragao, L. E. O. C., Ladle, R., Arai, E., Barbier, N., and Phillips, O.: Remote sensing detection of droughts in Amazonian forest canopies, The New Phytol., 187, 733–750, doi:10.1111/j.1469-8137.2010.03355.x, 2010.

Atkin, O. K. and Macherel, D.: The crucial role of plant mitochondria in orchestrating drought tolerance, Ann. Bot.-London, 103, 581–597, 2009.

Aubry-Kientz, M., Hérault, B., Ayotte-Trépanier, C., Baraloto, C., and Rossi, V.: Toward trait-based mortality models for tropical forests, PloS One, 8, e63678, doi:10.1371/journal.pone.0063678, 2013.

Baker, I. T., Prihodko, L., Denning, A. S., Goulden, M. L., Miller, S., and da Rocha, H. R.: Seasonal drought stress in the amazon: reconciling models and observations, J. Geophys. Res., 113, 2005–2012, doi:10.1029/2007JG000644, 2008.

Baraloto, C., Timothy Paine, C. E., Patino, S., Bonal, D., Herault, B., and Chave, J.: Functional trait variation and sampling strategies in species-rich plant communities, Funct. Ecol., 24, 208–216, 2009.

Beer, C., Reichstein, M., Tomelleri, E., Ciais, P., Jung, M., Carvalhais, N., Rodenbeck, C., Arain, M. A., Baldocchi, D., Bonan, G. B., Bondeau, A., Cescatti, A., Lasslop, G., Anders, L., Lomas, M., Luyssaert, S., Margolis, H., Olewson, K. W., Roupsard, O., Veenendaal, E., Viovy, N., Williams, C., Woodward, F. I., and Papale, D.: Terrestrial gross carbon dioxide uptake: global distribution and covariation with climate, Science, 329, 834–838, doi:10.1126/science.1184984, 2010.

Berry, J. A., Beerling, D. J., and Franks, P. J.: Stomata: key players in the earth system, past and present, Curr. Opin. Plant Biol., 13, 233–240, doi:10.1016/j.pbi.2010.04.013, 2010.

Betts, R. A., Boucher, O., Collins, M., Cox, P. M., Fallon, P. D., Gedney, N., Hemming, D. L., Huntingford, C., Jones, C., Sexton, D. M. H., and Webb, M. J.: Projected increase in continental runoff due to plant responses to increasing carbon dioxide, Nature, 448, 1037–1041, doi:10.1038/nature06045, 2007.

Booth, B. B. B., Jones, C., Collins, M., Totterdell, I. J., Cox, P. M., Sitch, S., Huntingford, C., Betts, R. A., Harris, G. R., and Lloyd, J.: High sensitivity of future global warming to land carbon cycle processes, Environ. Res. Lett., 7, 1–8, doi:10.1088/1748-9326/7/2/024002, 2012.

Calvet, J. C., Noilhan, J., Roujean, J. L., Bessemoulin, P., Cabelguenne, M., Olioso, A., and Wigneron, J. P.: An interactive vegetation SVAT model tested against data from six contrasting sites, Agr. Forest Meteorol., 92, 73–95, 1998.

Calvet, J. C., Rivalland, V., Picon-Cochard, C., and Guehl, J. M.: Modelling forest transpiration and CO_2 fluxes response to soil moisture stress, Agr. Forest Meteorol., 124, 143–156, 2004.

Carrer, D., Roujean, J. L., Lafont, S., Calvet, J. C., Boone, A., Decharme, B., Delire, C., and Gastellu-Etchegorry, J. P.: A canopy radiative transfer scheme with explicit FAPAR for the interactive vegetation model ISBA-A-gs: impact on carbon fluxes, J. Geophys. Res.-Biogeo., 118, 1–16, doi:10.1002/jgrg.20070, 2013.

Chen, B., Black, T. A., Coops, N. C., Hilker, T., Trofymow, J. A. T., and Morgenstern, K.: Assessing Tower Flux Footprint Climatology and Scaling Between Remotely Sensed and Eddy Covariance Measurements, Bound.-Lay. Meteorol., 130, 137–167, 2008.

Coe, M. T., Costa, M. H., and Soares-Filho, B. S.: The influence of historical and potential future deforestation on the stream flow of the Amazon River – land surface processes and atmospheric feedbacks, J. Hydrol., 369, 165–174, doi:10.1016/j.jhydrol.2009.02.043, 2009.

Cowling, S. A., Shin, Y., Pinto, E., and Jones, C. D.: Water recycling by Amazonian vegetation: coupled versus uncoupled vegetation–climate interactions, Phil. Trans. R. Soc. B, 363, 1865–1871, 2008.

Cox, P. M., Betts, R. A., Jones, C. D., Spall, S. A., and Totterdell, I. J.: Acceleration of global warming due to carbon-cycle feedbacks in a coupled climate model, Nature, 408, 184–187, 2000.

Cox, P. M., Betts, R. A., Collins, M., Harris, P. P., Huntingford, C., and Jones, C. D.: Amazonian forest dieback under climate-carbon cycle projections for the 21st century, Theor. Appl. Climatol., 78, 137–156, 2004.

da Costa, A. C. L., Galbraith, D., Almeida, S., Portela, B. T. T., da Costa, M., de Athaydes Silva Junior, J., Braga, A. P., de Gonçalves, P. H. L., de Oliveira, A. A. R., Fisher, R., Phillips, O. L., Metcalfe, D. B., Levy, P., and Meir, P.: Effect of 7 yr of experimental drought on the aboveground biomass storage of an eastern Amazonian rainforest, New Phytol., 187, 579–591, 2010.

Decharme, B., Douville, H., Boone, A., Habets, F., and Noilhan, J.: Impact of an exponential profile of saturated hydraulic conductivity within the ISBA LSM: simulations over the Rhone basin, J. Hydrometeorol., 7, 61–80, 2006

Decharme, B., Boone, A., Delire, C., and Noihlan, J.: Local evaluation of the Interaction between Soil Biosphere Atmosphere soil multilayer diffusion scheme using four pedotransfer functions, J. Geophys. Res., 116, 1984–2012, 2011.

Decharme, B., Martin, E., and Faroux, S.: Reconciling soil thermal and hydrological lower boundary conditions in land surface models, J. Geophys. Res.-Atmos., 118, 1–16, 2013.

De Kauwe, M., Medlyn, B. E., Zaehle, S., Walker, A. P., Dietze, M., Thomas, H., Jain, A. K., Luo, Y., Parton, W. J., Prentice, I. C., Smith, B., Thornton, P. E., Wang, S., Wang, Y.-P., Wårlind, D., Weng, E., Crous, K. Y., Ellsworth, D. S., Hanson, P. J., Seok Kim, H.-W., Jeffrey, M. W., Oren, R., and Norby, R. J.: Forest water use and water use efficiency at elevated CO_2: a model–data intercomparison at two contrasting temperate forest FACE sites, Glob. Change Biol., 19, 1759–1779, 2013.

Dickinson, R. E. and Henderson Sellers, A.: Modelling tropical deforestation: a study of GCM land surface parametrizations, Q. J. Roy. Meteor. Soc., 114, 439–462, 1988.

Domingues, T. F., Martinelli, L. A., and Ehleringer, J. R.: Ecophysiological traits of plant functional groups in forest and pasture ecosystems from eastern Amazonia, Brazil, Plant Ecol., 193, 101–112, 2007.

Douville, H., Ribes, A., Decharme, B., Alkama, R., and Sheffield, J.: Anthropogenic influence on multidecadal changes in reconstructed global evapotranspiration, Nature Climate Change, 3, 59–62, 2013.

Egea, G., Verhoef, A., and Vidale, P. L.: Towards an improved and more flexible representation of water stress in coupled photosynthesis–stomatal conductance models, Agr. Forest Meteorol., 151, 1370–1384, 2011.

Eltahir, E. and Bras, R. L.: Precipitation recycling in the Amazon Basin, Q. J. Roy. Meteor. Soc., 120, 861–880, 1994.

Fisher, R. A., Williams, M., Do Vale, R. L., Da Costa, A. L., and Meir, P.: Evidence from Amazonian forest is consistent with isohydric control of leaf water potential, Plant Cell Environ., 29, 151–165, 2006.

Fisher, R. A., Williams, M., da Costa, A. L., Malhi, Y., da Costa, R. F., Almeida, S., and Meir, P.: The response of an Eastern Amazonian rain forest to drought stress: results and modelling analyses from a throughfall exclusion experiment, Glob. Change Biol., 13, 2361–2378, 2007.

Fisher, R. A., McDowell, N., Purves, D., Moorcroft, P., Sitch, S., Cox, P., Huntingford, C., Meir, P., and Woodward, F. I.: Assessing uncertainties in a second-generation dynamic vegetation model due to ecological scale limitations, New Phytol., 187, 666–681, 2010.

Friedlingstein, P., Cox, P., Betts, R., Bopp, L., von Bloh, W., Brovkin, V., Cadule, P., Doney, S., Eby, M., Fung, I., Bala, G., John, J., Jones, C., Joos, F., Kato, T., Kawamiya, M., Knorr, W., Lindsay, K., Matthews, H. D., Raddatz, T., Rayner, P., Reick, C., Roeckner, E., Schnitzler, K. G., Schnur, R., Strassmann, K.,Weaver, A. J., Yoshikawa, C., and Zeng, N.: Climate-carbon cycle feedback analysis: results from the C4MIP model intercomparison, J. Climate, 19, 3337–3353, 2006.

Fu, R., Yin, L., Li, W., Arias, P. A., Dickinson, R. E., Huang, L., Chakraborty, S., Fernandes, K., Liebmann, B., Fisher, R. A., and Myneni, R. B.: Increased dry-season length over southern Amazonia in recent decades and its implication for future climate projection, P. Natl. Acad. Sci. USA, 110, 18110–18115, doi:10.1073/pnas.1302584110, 2013.

Galbraith, D., Levy, P. E., Sitch, S., Huntingford, C., Cox, P., Williams, M., and Meir, P.: Multiple mechanisms of Amazonian forest biomass losses in three dynamic global vegetation models under climate change, New Phytol., 187, 647–665, 2010.

Gatti, L. V., Gloor, M., Miller, J. B., Doughty, C. E., Malhi, Y., Domingues, L. G., Basso, L. S., Martinewski, A., Correia, C. S. C., and Borges, V. F.: Drought sensitivity of Amazonian carbon balance revealed by atmospheric measurements, Nature, 506, 76–80, 2014.

Gedney, N., Cox, P. M., Betts, R. A., Boucher, O., Huntingford, C., and Stott, P. A.: Detection of a direct carbon dioxide effect in continental river runoff records, Nature, 439, 835–838, 2006.

Gibelin, A. L., Calvet, J. C., Roujean, J. L., Jarlan, L., and Los, S. O.: Ability of the land surface model ISBA-A-gs to simulate leaf area index at the global scale: comparison with satellites products, J. Geophys. Res., 111, 1984–2012, 2006.

Gibelin, A. L., Calvet, J. C., and Viovy, N.: Modelling energy and CO_2 fluxes with an interactive vegetation, land surface model, Evaluation at high and middle latitudes, Agr. Forest Meteorol., 148, 1611–1628, 2008.

Good, P., Jones, C., Lowe, J., Betts, R., and Gedney, N.: Comparing tropical forest projections from two generations of Hadley Centre Earth System models, HadGEM2-ES and HadCM3LC, J. Climate, 26, 495–511, 2013.

Guimberteau, M., Ducharne, A., Ciais, P., Boisier, J. P., Peng, S., De Weirdt, M., and Verbeeck, H.: Testing conceptual and physically based soil hydrology schemes against observations for the Amazon Basin, Geosci. Model Dev., 7, 1115–1136, doi:10.5194/gmd-7-1115-2014, 2014.

Huntingford, C., Zelazowski, P., Galbraith, D., Mercado, L. M., Sitch, S., Fisher, R. A., Lomas, M., Walker, A. P., Jones, C. D., Booth, B. B. B., Malhi, Y., Hemming, D., Kay, G., Good, P., Lewis, S.L., Phillips, O. L., Atkin, O. K., Lloyd, J., Gloor, E., Zaragoza-Castells, J., Meir, P., Betts, R., Harris, P. P, Nobre, C., Marengo, C., and Cox, P. M.: Simulated resilience of tropical rainforests to CO_2-induced climate change, Nat. Geosci., 6, 268–273, 2013.

Jacobs, C. M. J.: Direct impact of atmospheric CO_2 enrichment on regional transpiration, Ph.D. thesis, Agricultural University, Wageningen, 1995.

Joetzjer, E., Douville, H., Delire, C., and Ciais, P.: Present-day and future Amazonian precipitation in global climate models: CMIP5 versus CMIP3, Clim. Dynam., 41, 2921–2936, 2013.

Jupp, T. E., Cox, P. M., Rammig, A., Thonicke, K., Lucht, W., and Cramer, W.: Development of probability density functions for future South American rainfall, New Phytol., 187, 682–693, 2010.

Keenan, T. F., Hollinger, D. Y., Bohrer, G., Dragoni, D., Munger, J. W., Schmid, H. P., and Richardson, A. D.: Increase in forest water-use efficiency as atmospheric carbon dioxide concentrations rise, Nature, 499, 324–327, doi:10.1038/nature12291, 2013.

Lewis, S. L., Brando, P. M., Phillips, O. L., van der Heijden, G. M., and Nepstad, D.: The 2010 Amazon drought, Science, 331, 554–554, doi:10.1126/science.1200807, 2011.

Lloyd, J. and Farquhar, G. D.: Effects of rising temperatures and [CO_2] on the physiology of tropical forest trees, Philos. T. R. Soc. B, 363, 1811–1817, 2008.

Malhi, Y., Wood, D., Baker, T. R., Wright, J., Phillips, O. L., Cochrane, T., Meir, P., Chave, J., Almeida, S., Arroyo, L., Higuchi, N., Killeen, T. J., Laurance, S. G., Laurance, W. F., Lewis, S. L., Monteagudo, A., Neill, D. A., Núñez Vargas, P., Pitman, N. C. A., Quesada, C. A., Salomão, R., Silva, J. N. M., Torres Lezama, A., Terborgh, J., Vásquez Martínez, R., and Vinceti, B.: The regional variation of aboveground live biomass in old-growth Amazonian forests, Glob. Change Biol., 12, 1107–1138, 2006.

Malhi, Y., Roberts, J. T., Betts, R. A., Killeen, T. J., Li, W., and Nobre, C. A.: Climate change, deforestation, and the fate of the Amazon, Science, 319, 169–172, 2008.

Malhi, Y., Aragao, L. E. O., Metcalfe, D. B., Paiva, R., Quesada, C. A., Almeida, S., Anderson, L., Brando, P., Chamber, J. Q., and da Costa, A. C. L.: Comprehensive assessment of carbon productivity, allocation and storage in three Amazonian forests, Glob. Change Biol., 15, 1255–1274, 2009.

Markewitz, D., Devine, S., Davidson, E. A., Brando, P., and Nepstad, D. C.: Soil moisture depletion under simulated drought in the Amazon: impacts on deep root uptake, New Phytol., 187, 592–607, 2010.

McDowell, N. G., Beerling, D. J., Breshears, D. D., Fisher, R. A., Raffa, K. F., and Stitt, M.: The interdependence of mechanisms underlying climate-driven vegetation mortality, Trends Ecol. Evol., 26, 523–532, 2011.

McDowell, N. G., Fisher, R. A., Xu, C., Domec, J. C., Holtta, T., Mackay, S., Sperry, J. S., Boutz, A., Dickman, L., and Gehres, N.: Evaluating theories of drought-induced vegetation mortality using a multimodel–experiment framework, New Phytol., 200, 304–321, 2013.

Meir, P., Cox, P., and Grace, J.: The influence of terrestrial ecosystems on climate, Trends Ecol. Evol., 21, 254–260, 2006.

Meir, P., Metcalfe, D. B., Costa, A. C. L., and Fisher, R. A.: The fate of assimilated carbon during drought: impacts on respiration in Amazonian rainforests, Philos. T. R. Soc. B, 363, 1849–1855, 2008.

Meir, P., Brando, P. M., Nepstad, D., Vasconcelos, S., Costa, A. C. L., Davidson, E., Almeida, S., Fisher, R. A., Sotta, E. D., and Zarin, D.: The effects of drought on Amazonian rain forests, in: Amazonia and global change, edited by: Keller, M., Bustamante, M., Gash, J., and Silva Dias, P., Geoph. Monog. Series, 186, 429–449, 2009.

Metcalfe, D. B., Meir, P., Aragao, L. E. O. C., Lobo-do-Vale, R., Galbraith, D., Fisher, R. A., Chaves, M. M., Maroco, J. P., da Costa, A. C. L., de Almeida, S. S., Braga, A. P., Gonçalves, P. H. L, de Athaydes, J., da Costa, M., Portela, T. T. B., de Oliveira, A. A. R., Malhi, and Williams, M.: Shifts in plant respiration and carbon use efficiency at a large-scale drought experiment in the eastern Amazon, New Phytol., 187, 608–621, 2010.

Miranda, E. J., Vourlitis, G. L., Filho, N. P., Priante, P. C., Campelo, J. H., Suli, G. S., Fritzen, C. L., De Almeida Lobo, F., and Shiraiwa, S.: Seasonal variation in the leaf gas exchange of tropical forest trees in the rain forest–savanna transition of the southern Amazon basin, J. Trop. Ecol., 21, 451–460, 2005.

Nepstad, D. C., Moutinho, P., Dias, M. B., Davidson, E., Cardinot, G., Markewitz, D., Figueiredo, R., Vianna, N., Chambers, J., Ray, D., Guerreiros, J. B., Lefebvre, P., Sternberg, L., Moreira, M., Barros, L., Ishida, F. Y., Tohlver, I., Belk, E., Kalif, K., and Schwalbe, K.: The effects of partial throughfall exclusion on canopy processes, aboveground production and biogeochemistry of an Amazon forest, J. Geophys. Res.-Atmos., 107, 1–18, 2002.

Nepstad, D. C., Lefebvre, P., Lopes da Silva, U., Tomasella, J., Schlesinger, P., Solorzano, L., Moutinho, P., Ray, D., and Guerreira Benito, J.: Amazon drought and its implications for forest flammability and tree growth: a basin-wide analysis, Glob. Change Biol., 10, 704–717, 2004.

Nepstad, D. C., Tohver, I. M., Ray, D., Moutinho, P., and Cardinot, G.: Mortality of large trees and lianas following experimental drought in an Amazon forest, Ecology, 88, 2259–2269, 2007.

Pan, Y., Birdsey, R. A., Fang, J., Houghton, R., Kauppi, P. E., Kurz, W. A., Phillips, O. L., Shvidenko, A., Lewis, S. L., Canadell, J. G., Ciais, P., Jackson, R. B., Pacala, S. W., McGuire, A. D., Piao, S., Rautiainen, A., Sitch, S., and Hayes, D.: A large and persistent carbon sink in the world's forests, Science, 333, 988–993, 2011.

Phillips, O. L., Aragao, L. E. O. C., Lewis, S. L., Fisher, J. B., Lloyd, J., Lopez-Gonzalez, G., Malhi, Y., Monteagudo, A., Peacock, J., Quesada, C. A., van der Heijden, G., Almeida, S., Amaral, I., Arroyo, L., Aymard, G., Baker, T. R., Banki, O., Blanc, L., Bonal, D., Brando, P., Chave, J., Alves de Oliveira, A. C., Cardozo, N. D., Czimczik, C. I., Feldpausch, T. R., Freitas, M. A., Gloor, E., Higuchi, N., Jimenez, E., Lloyd, G., Meir, P., Mendoza, C., Morel, A., Neill, D. A., Nepstad, D., Patino, S., Cristina Penuela, M., Prieto, A., Ramirez, F., Schwarz, M., Silva, J., Silveira, M., Thomas, A. S., ter Steege, H., Stropp, J., Vasquez, R., Zelazowski, P., Alvarez Davila, E., Andelman, S., Andrade, A., Chao, K.-J., Erwin, T., Di Fiore, A., Honorio C, E., Keeling, H., Killeen, T. J., Laurance, W. F., Pena Cruz, A., Pitman, N. C. A., Nunez Vargas, P., Ramirez-Angulo, H., Rudas, A., Salamao, R., Silva, N., Terborgh, J., and Torres-Lezama, A.: Drought sensitivity of the Amazon rainforest, Science, 323, 1344–1347, 2009.

Phillips, O. L., Van Der Heijden, G., Lewis, S. L., Lopez-Gonzalez, G., Aragao, L. E. O. C., Lloyd, J., Malhi, Y., Monteagudo, A., Almeida, S., Davila, E. A., Amaral, I., Andelman, S., Andrade, A., Arroyo, L., Aymard, G., Baker, T. R., Blanc, L., Bonal, D., De Oliveira, A. C. A., Chao, K.-J., Cardozo, N. D., Da Costa, L., Feldpausch, T. R., Fisher, J. B., Fyllas, N. M., Freitas, M. A., Galbraith, D., Gloor, E., Higuchi, N., Honorio, E., Jimenez, E., Keeling, H., Killeen, T. J., Lovett, J. C., Meir, P., Mendoza, C., Morel, A., Vargas, P. N., Patino, S., Peh, K. S. H., Cruz, A. P., Prieto, A., Quesada, C. A., Ram?rez, F., Ram?rez, H., Rudas, A., Salamao, R., Schwarz, M., Silva, J., Silveira, M., Ferry Slik, J. W., Sonke, B., Thomas, A. S., Stropp, J., Taplin, J. R. D., Vasquez, R., Vilanova, E.: Drought–mortality relationships for tropical forests, New Phytol., 187, 631–646, 2010.

Picon, C., Guehl, J. M., and Ferhi, A.: Leaf gas exchange and carbon isotope composition responses to drought in a drought – avoiding (*Pinus pinaster*) and a drought-tolerant (*Quercus petraea*) species under present and elevated atmospheric CO_2 concentrations, Plant Cell Environ., 19, 182–190, 1996.

Potter, C. S. and Klooster, S. A.: Detecting a terrestrial biosphere sink for carbon dioxide: interannual ecosystem modeling for the mid 1980s, Climatic Change, 42, 489–503, 1999.

Poulter, B., Heyder, U., and Cramer, W.: Modeling the sensitivity of the seasonal cycle of GPP to dynamic LAI and soil depths in tropical rainforests, Ecosystems, 12, 517–533, 2009.

Powell, T. L., Galbraith, D. R., Christoffersen, B. O., Harper, A., Imbuzeiro, H. M. A., Rowland, L., Almeida, S., Brando, P. M., da Costa, A. C. L., Costa, M. H., Levine, N. M., Malhi, Y., Saleska, S. R., Sotta, E., Williams, M., Meir, P., and Moorcroft, P.: Confronting model predictions of carbon fluxes with measurements of Amazon forests subjected to experimental drought, New Phytol., 200, 350–365, 2013.

Rammig, A., Jupp, T., Thonicke, K., Tietjen, B., Heinke, J., Ostberg, S., Lucht, W., Cramer, W., and Cox, P.: Estimating the risk of Amazonian forest dieback, New Phytol., 187, 694–706, 2010.

Reichstein, M., Bahn, M., Ciais, P., Frank, D., Mahecha, M. D., Seneviratne, S. I., Zscheischler, J., Beer, C., Buchmann, N., Frank, D. C., Papale, D., Rammig, A., Smith, P., Thon- icke, K., van der Velde, M., Vicca, S., Walz, A., and Wattenbach, M.: Climate extremes and the carbon cycle, Nature, 500, 287–295, 2013.

Ruivo, M. L. P. and Cunha, E. S.: Mineral and organic components in archaeological black earth and yellow latosol in Caxiuanã, Amazon, Brazil, Adv. Ecol. Sci., 18, 1113–1121, 2003.

Sakaguchi, K., Zeng, X., Christoffersen, B. J., Restrepo-Coupe, N., Saleska, S. R., and Brando, P. M.: Natural and drought scenarios in an east central Amazon forest: fidelity of the Community Land Model 3.5 with three biogeochemical models, J. Geophys. Res., 116, G01029, doi:10.1029/2010JG001477, 2011.

Shiogama, H., Emori, S., Hanasaki, N., Abe, M., Masutomi, Y., and Takahashi, K.: Observational constraints indicate risk of drying in the Amazon basin, Nature Communications, 3, 253–257, doi:10.1038/ncomms1252, 2011.

Sotta, E. D., Veldkamp, E., Schwendenmann, L., Guimaraes, B. R., Paixao, R. K., Ruivo, M. L. P., da Costa, A. C. L., and Meir, P.: Effects of an induced drought on soil carbon dioxide (CO_2) efflux and soil CO_2 production in an eastern Amazonian rainforest, Brazil, Glob. Change Biol., 13, 2218–2229, 2007.

Van der Molen, M. K., Dolman, A. J., Ciais, P., Eglin, T., Gobron, N., Law, B. E., Meir, P., Peters, W., Phillips, O. L., Reichstein, M., Chen, T., Dekker, S. C., Doubková, M., Friedl, M. A., Jung, M., van den Hurk, B. J. J. M., de Jeu, R. A. M., Kruijt, B., Ohta, T., Rebel, K. T., Plummer, S., Seneviratne, S. I., Sitch, S., Teuling, A. J., van der Werf, G. R., and Wang, G.: Drought and ecosystem carbon cycling, Agr. Forest Meteorol., 151, 765–773, 2011.

Verbeeck, H., Peylin, P., Bacour, C., Bonal, D., Steppe, K., and Ciais, P.: Seasonal patterns of CO2fluxes in Amazon forests: fusion of eddy covariance data and the ORCHIDEE model, J. Geophys. Res., 116, G02018, doi:10.1029/2010JG001544, 2011.

Williams, M., Bond, B. J., and Ryan, M. G.: Evaluating different soil and plant hydraulic constraints on tree function using a model and sap flow data from ponderosa pine, Plant Cell Environ., 24, 679–690, 2001.

Woodward, F. I.: Climate and Plant Distribution, Cambridge University Press, 1987.

Zeppel, M., Macinnis-Ng, C., Palmer, A., Taylor, D., Whitley, R., Fuentes, S., Yunusa, I., Williams, M., and Eamus, D.: An analysis of the sensitivity of sap flux to soil and plant variables assessed for an Australian woodland using SPA, Funct. Plant Biol., 35, 509–520, 2008.

Zhou, S., Duursma, R., Medlyn, B. E., Kelley, J. W. G., and Prentice, I. C.: How should we model plant responses to drought? An analysis of stomatal and non-stomatal responses to water stress, Agr. Forest Meteorol., 182–183,204–214, 2013.

Title Page

Abstract | Introduction

Conclusions | References

Tables | Figures

◀| |▶

◀ ▶

Back | Close

Full Screen / Esc

Printer-friendly Version

Interactive Discussion

Table 1. ISBA$_{\mathrm{CC}}$: nomenclature and main equations.

Symbols	Units	Description	
A_m	$\mathrm{kg_{CO_2}\,m^{-2}\,s^{-1}}$	Photosynthesis rate (light saturated)	
C_a	ppmv	Atmospheric CO$_2$ concentration	
C_i	ppmv	Leaf internal CO$_2$ concentration	
D_s	$\mathrm{g\,kg^{-1}}$	Saturation deficit at the leaf surface	
D_max	$\mathrm{g\,kg^{-1}}$	Maximum value of D_s	
f	unitless	coupling factor	
f_0	unitless	coupling factor at saturating air humidity ($D_\mathrm{s} = 0$)	
f_0^*	unitless	coupling factor in well-watered conditions and at saturating air humidity ($D_\mathrm{s} = 0$)	
f_min	unitless	coupling factor at maximum air humidity deficit ($D_\mathrm{s} = D_\mathrm{max}$)	
Γ	ppmv	CO$_2$ concentration compensation point	
g_m	$\mathrm{mm\,s^{-1}}$	Mesophyll conductance defined as the light saturated rate of photosynthesis (Jacobs, 1995)	
g_m^*	$\mathrm{mm\,s^{-1}}$	g_m in well-watered conditions	
g_s	$\mathrm{mm\,s^{-1}}$	Stomatal conductace	
Equations			
$g_\mathrm{m}^* = \frac{A_\mathrm{m}}{C_\mathrm{i}-\Gamma}$			(1)
$f = \frac{C_\mathrm{i}-\Gamma}{C_\mathrm{a}-\Gamma}$			(2)
$f = f_0 \cdot \left(1 - \frac{D_\mathrm{s}}{D_\mathrm{max}}\right) + f_\mathrm{min} \cdot \frac{D_\mathrm{s}}{D_\mathrm{max}}$			(3)

Table 2. Description of ISBA_{CC}: water stress functions.

Name	Conditions SWI	Water Stress functions applied to g_m	Water Stress functions applied to f_0	References
Avoiding	$\text{SWI} \geq 1$	$\ln(g^*_\text{m}) = 4.7 - 7.f^*_0$		Calvet et al. (2004)
	$\text{SWIc} < \text{SWI} < 1$	$g_\text{m} = g^*_\text{m}$	$f_0 = f^*_0 - (f^*_0 - f^N_0)\frac{(1-\text{SWI})}{(1-\text{SWIc})}$	
	$\text{SWI} \leq \text{SWIc}$	$g_\text{m} = g^*_\text{m} \cdot \frac{\text{SWI}}{\text{SWIc}}$	$f_0 = \frac{2.8-\ln(g_\text{m})}{7}$	
Tolerant	$\text{SWI} \geq 1$	$\ln(g^*_\text{m}) = 4.7 - 7.f^*_0$		Calvet et al. (2004)
	$\text{SWIc} < \text{SWI} < 1$	$g_\text{m} = g^*_\text{m} - (g^*_\text{m} - g^N_\text{m}) \cdot \frac{(1-\text{SWI})}{(1-\text{SWIc})}$	$f_0 = f^*_0$	
	$\text{SWI} \leq \text{SWIc}$	$g_\text{m} = g^N_\text{m} \cdot \frac{\text{SWI}}{\text{SWIc}}$	$f_0 = \frac{2.8-\ln(g_\text{m})}{7}$	
Linear		$g_\text{m} = \text{SWI} \cdot g^*_\text{m}$	$f_0 = 0.74$	Domingues et al. (2007)
SiB3		$g_\text{m} = \frac{(1+\alpha) \cdot SWI}{(\alpha \cdot SWI)} \cdot g^*_\text{m}$; $\alpha = 0.1$ Domingues et al. (2007)	$f_0 = 0.74$	Harper et al. (2013)
Symbol	Description			
SWIc	Critical extractable soil moisture content (drought-avoiding and tolerant)			$\text{SWIc} = 0.3$
f^N_0	Minimum value of f_0 at $\text{SWI} = \text{SWIc}$ (drought-avoiding)			$f^N_0 = \frac{\ln(g^*_\text{m})-2.8}{7}$
g^N_m	Value of g_m at $\text{SWI} = \text{SWIc}$ in $\text{mm}\,\text{s}^{-1}$ (drought-tolerant)			$\ln(g^N_\text{m}) = 2.8 - 7.f^*_0$

Table 3. Observations used in this study.

Observations	Symbol	Units	Tapajos	Caxiuanã
Soil Water Content	SWC	$\mathrm{m^3\,m^{-3}}$	1999–2005 Brando et al. (2008) Markewitz et al. (2010)	2001–2004 Fisher et al. (2007)
Stomatal Conductance	g_s	$\mathrm{mmol_{CO_2}\,m^{-2}\,s^{-1}}$		2002–2003 Fisher et al. (2006)
Sap Flow	SF	$\mathrm{mm\,day^{-1}}$		2002–2003 Fisher et al. (2006)
Evapotranspiration	ET	$\mathrm{mm\,day^{-1}}$	1999–2004 (modeled) Markewitz et al. (2010)	
Gross Primary Production	GPP	$\mathrm{\mu mol_{CO_2}\,m^{-2}\,s^{-1}}$		2002–2003 (modeled) Fisher et al. (2007)
Ecosystem Respiration	R_e	$\mathrm{t_C\,ha^{-1}\,yr^{-1}}$		2001–2005 Metcalfe et al. (2010)
Autotrophic Respiration	R_a	$\mathrm{t_C\,ha^{-1}\,yr^{-1}}$		2001–2005 Metcalfe et al. (2010)
Leaf Respiration	R_l	$\mathrm{t_C\,ha^{-1}\,yr^{-1}}$		2001–2005 Metcalfe et al. (2010)
Wood Respiration	R_w	$\mathrm{t_C\,ha^{-1}\,yr^{-1}}$		2001–2005 Metcalfe et al. (2010)
Root Respiration	R_r	$\mathrm{t_C\,ha^{-1}\,yr^{-1}}$		2001–2005 Metcalfe et al. (2010)
Soil Respiration	R_s	$\mathrm{t_C\,ha^{-1}\,yr^{-1}}$	1999–2004 Davidson et al. (2008)	2001–2005 Metcalfe et al. (2010)
Leaf Area Index	LAI	$\mathrm{m^2\,m^{-2}}$	2000–2005 Brando et al. (2008)	2001–2007 Fisher et al. (2007)
Above Ground Biomasse	AGB	$\mathrm{t_C\,ha^{-1}\,yr^{-1}}$	1999–2005 Brando et al. (2008)	2000–2008 Da Costa (2010)

Table 4. Summary of the experiments.

Forcing	Tolerant	Avoiding	Linear	SiB3	sites
in situ	×	×	×	×	Caxiuanã and Tapajos
in situ + 4 °C			×	×	Caxiuanã
in situ $\times 4[CO_2]$			×	×	Caxiuanã
in situ + 4 °C $\times 4[CO_2]$			×	×	Caxiuanã

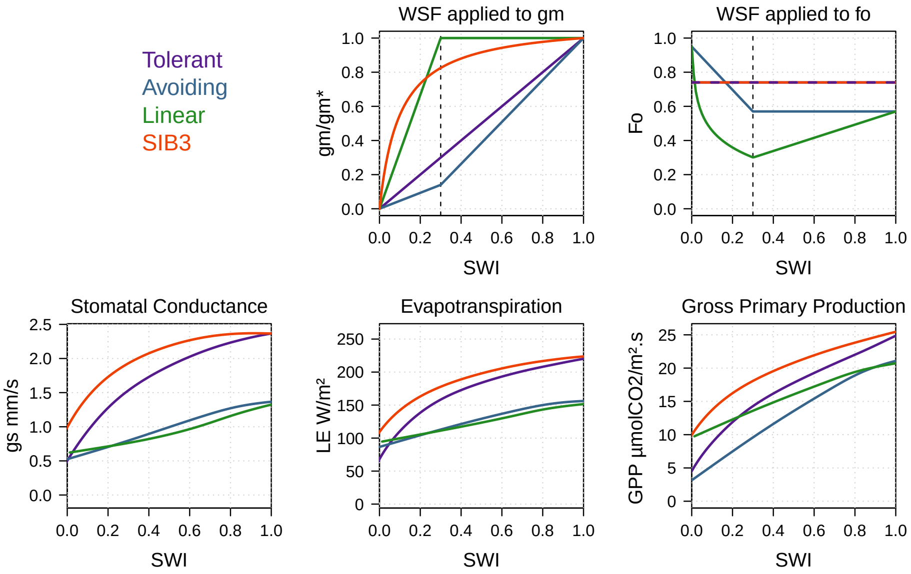

Figure 1. Graphical representation of the mesophyll conductance (gm),the coupling factor at saturating air humidity (f_0), the stomatal conductance (g_s), the evapotranspiration (LE) and the Gross Primary Production (GPP) for the four Water Stress Functions (WSF) used in this study against the Soil Wetness Index (SWI).

Title Page
Abstract
Introduction
Conclusions
References
Tables
Figures
◀▌
▐▶
◀
▶
Back
Close
Full Screen / Esc
Printer-friendly Version
Interactive Discussion

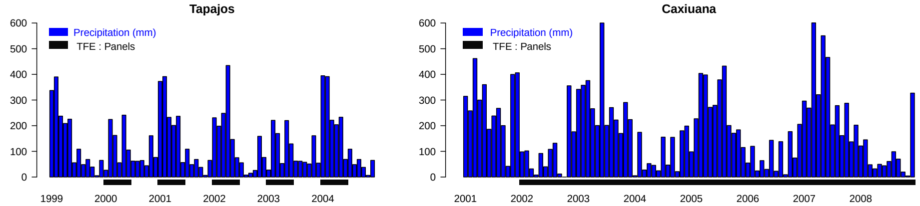

Figure 2. Monthly observed precipitation at Tapajos and Caxiuanã. Horizontal black bars indicate when panels were applied for the TFE experiments.

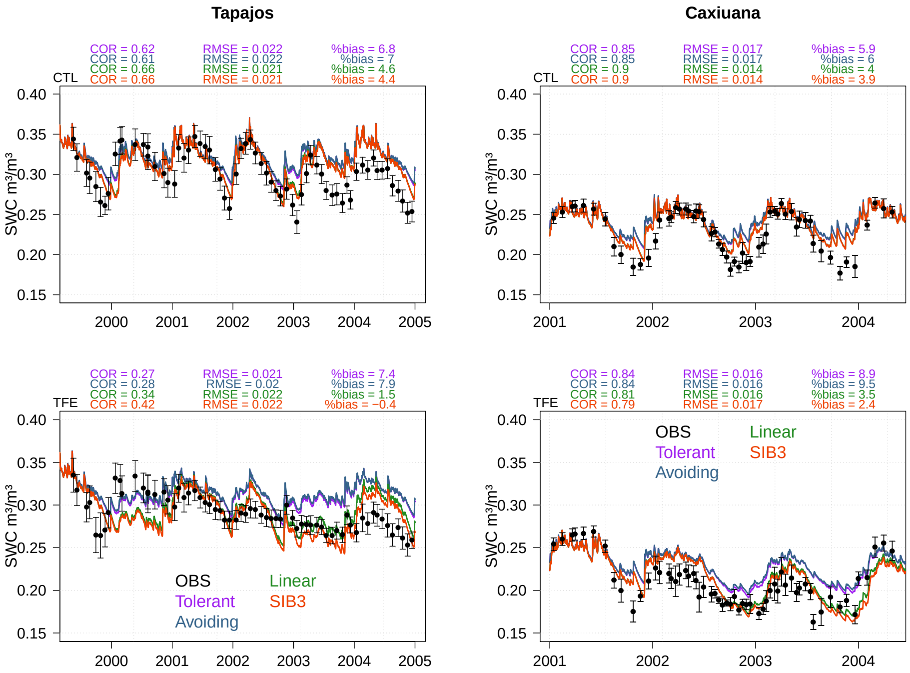

Figure 3. Daily observed and simulated Soil Water Content with the 4 WSF at Tapajos (left) and Caxiuanã (right) for both CTL (top) and TFE (bottom) plots. The SWC measured at the TFE plots were rescaled to have identical SWC than the CTL plots during the baseline year.

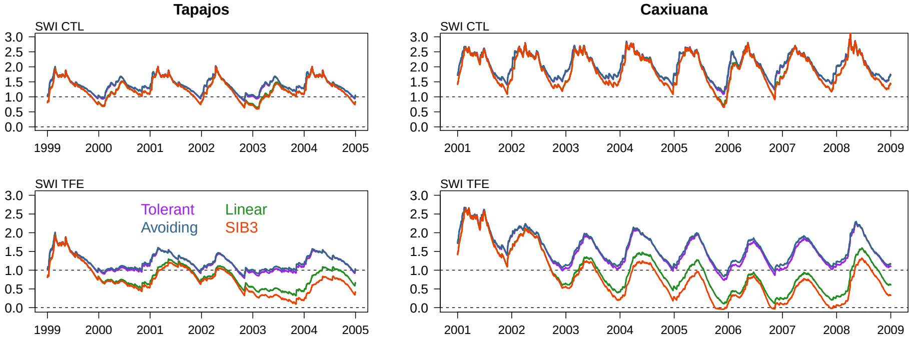

Figure 4. Simulated daily Soil Wetness Index (SWI) with the 4 WSF at Tapajos (left) and Caxiuanã (right) for both CTL (top) and TFE for the full experimental period.

Title Page
Abstract
Introduction
Conclusions
References
Tables
Figures
◀◀
▶▶
◀
▶
Back
Close
Full Screen / Esc
Printer-friendly Version
Interactive Discussion

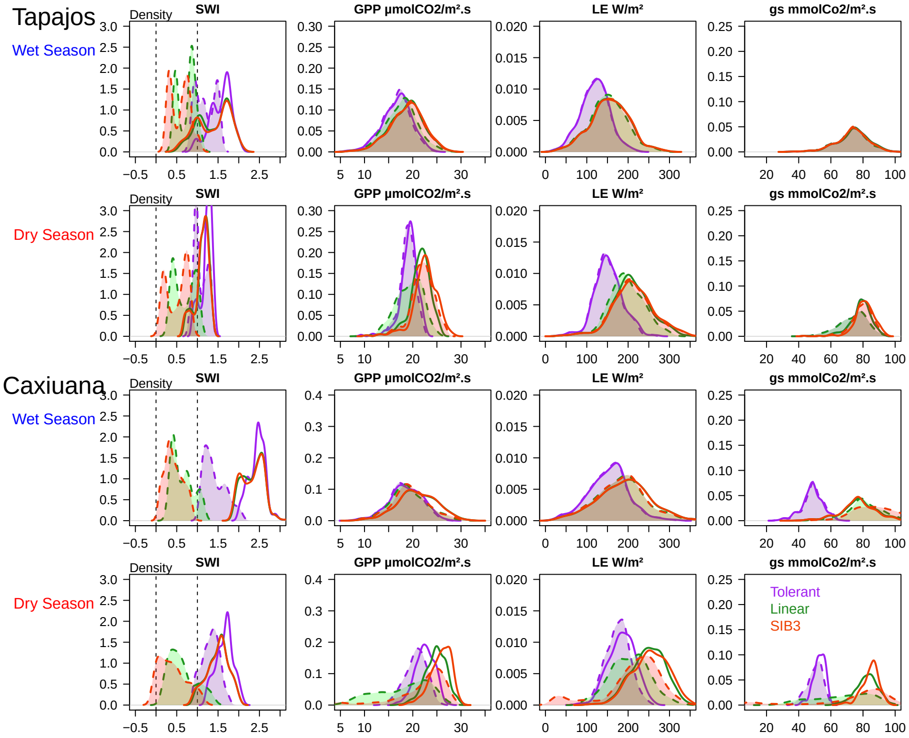

Figure 5. Probability density functions of the daily Soil Wetness Index (SWI), Gross Primary Production (GPP), Evapotranspiration (LE) and the stomatal conductance (g_s), for the Tolerant, Linear and SIB3 WSF, calculated for the Dry season (from August to October) and the wet season (from February to April) during the treatment period (i.e. baseline year excluded) at Caxiuanã and Tapajos. Solid lines indicates the CTL plots and dashed lines and shaded areas the TFE plots. The daily means are calculated for incoming short wave radiation > 100 W m^{-2}.

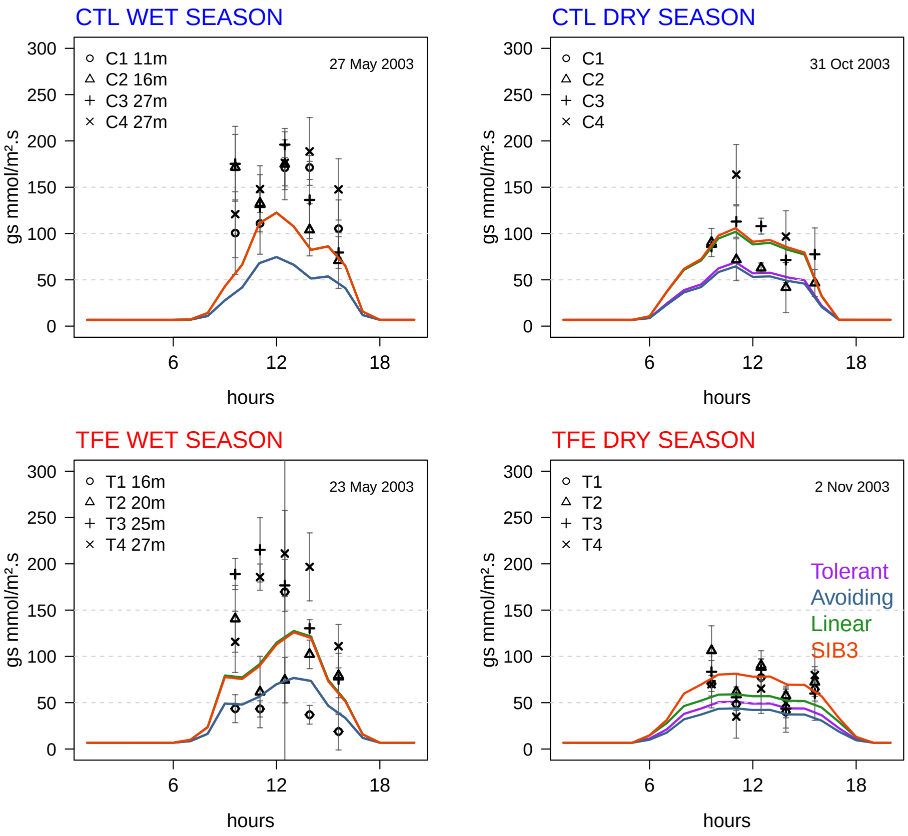

Figure 6. Seasonal variability of the hourly observed (symbols C1–C4 are trees in the control plot and T1–T4 are trees in the TFE plot) and simulated stomatal conductance with the 4 WSF (lines) at Caxiuanã.

Title Page
Abstract
Introduction
Conclusions
References
Tables
Figures
◀|
|▶
◀
▶
Back
Close
Full Screen / Esc
Printer-friendly Version
Interactive Discussion

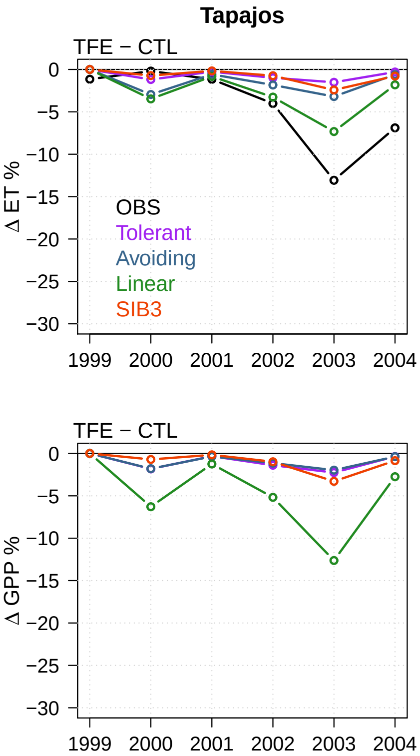

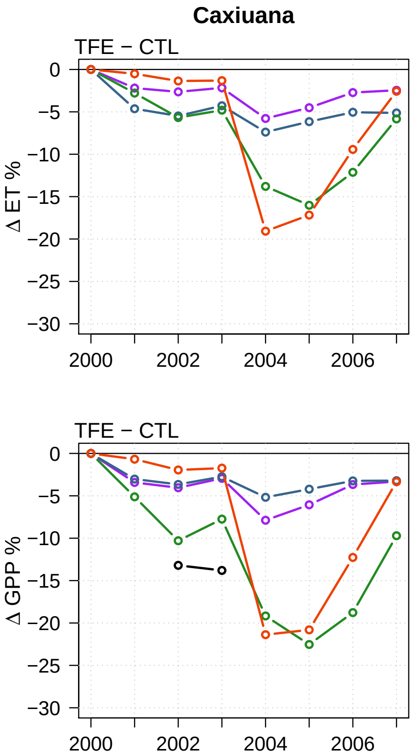

Figure 7. Annual mean differences (TFE plot minus CTL plot) in simulated ET (top) with ISBACC and Markewitz's model outputs as proxy (Markewitz et al., 2010). Annual differences (exclusion plot minus control plot) in simulated GPP (bottom) with ISBACC and SPA's model outputs as proxy (Fisher et al., 2007).

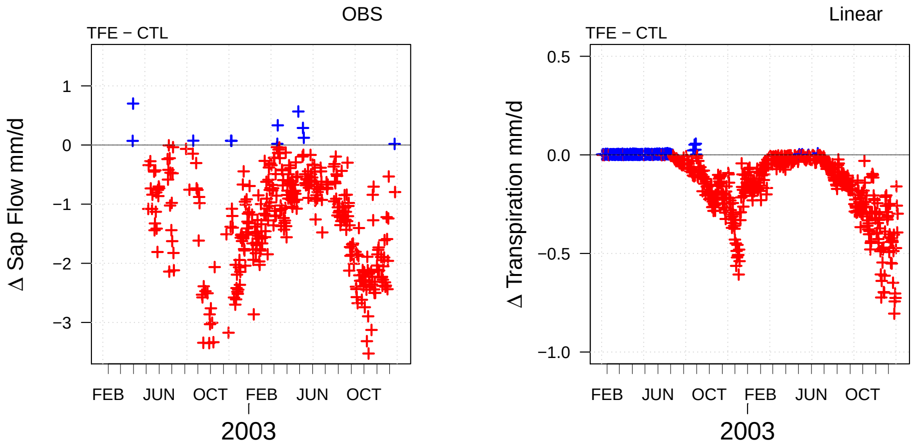

Figure 8. Difference (TFE plot minus CTL plot (Δ)) in daily observed sap flow and simulated transpiration at Caxiuanã from february 2002 to December 2003. Red crosses indicate Δ < 0 while blue crosses indicate Δ > 0.

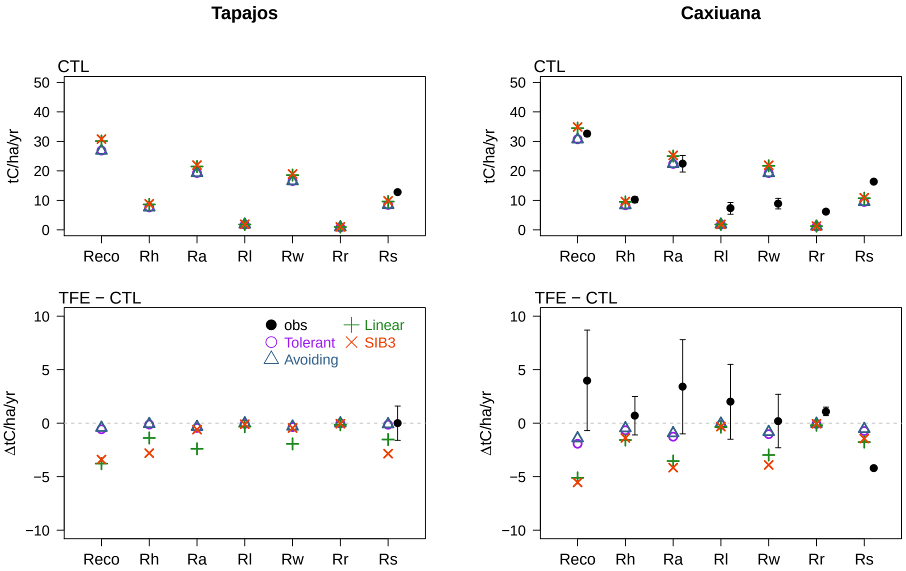

Figure 9. Annual Ecosystem (Re), Heterotrophic (Rh), Autotrophic (Ra), Leaf (Rl), Wood (Rw), Root (Rr) and Soil (Rs) respirations for the fourth year of the experiment for the control plot (top) and the difference between the exclusion and control plot (bottom) at Tapajos (left) and Caxiuanã (right).

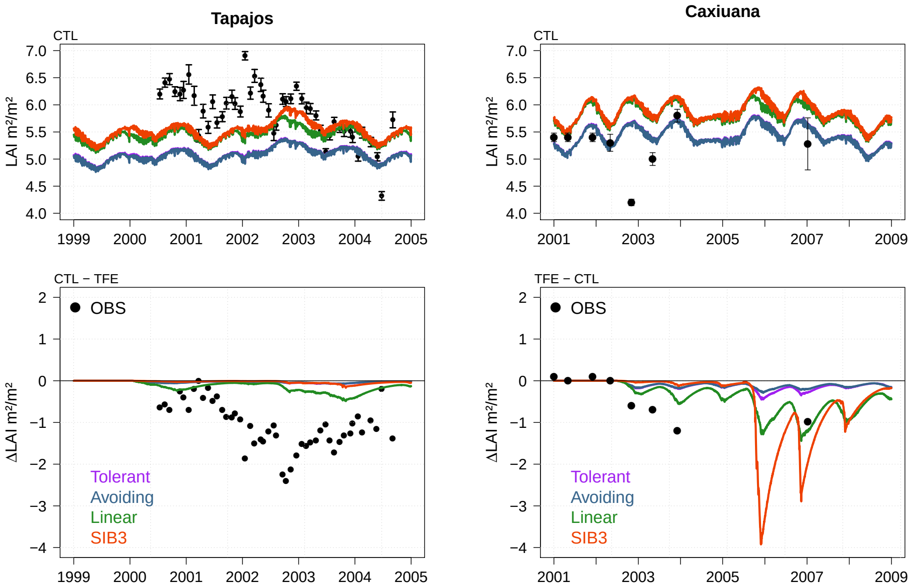

Figure 10. Times series of the daily Leaf Area Index (LAI) for the control plot (top) and the difference between the exclusion and control plot (bottom) at Tapajos (left) and Caxiuanã (right).

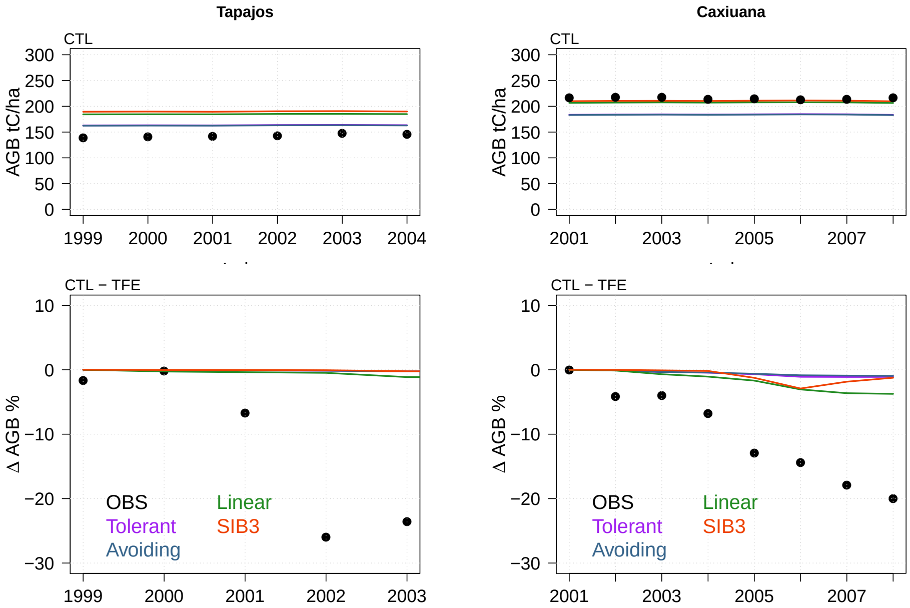

Figure 11. Times series of the yearly Above Ground Biomass (AGB) for the control plot (top) and the difference between the exclusion and control plot (bottom) at Tapajos (left) and Caxiuanã (right).

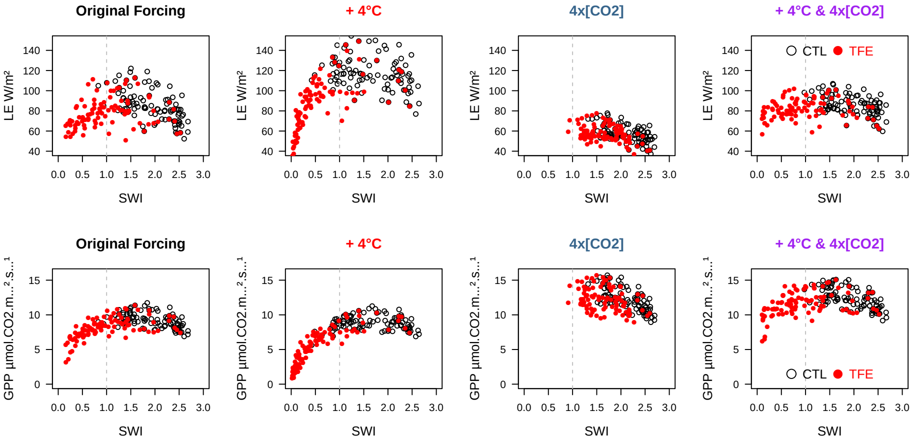

Figure 12. Simulated monthly LE and GPP vs. monthly SWI using the Linear WSF, under undisturbed and disturbed meteorological forcings for both CTL (black empty dots) and TFE (red full dots) plots at Caxiuanã.